NASA CR-167393

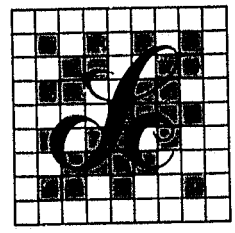

LinCom Corporation
P.O. Box 2793D, Pasadena, Calif. 91105

LinCom

SOLAR POWER SATELLITE ANTENNA PHASE CONTROL SYSTEM

HARDWARE SIMULATION PHASE IV

VOLUME I. EXECUTIVE SUMMARY

PREPARED BY

NASA LYNDON B. JOHNSON SPACE CENTER
HOUSTON, TX 77058

TECHNICAL MONITOR: JACK SEYL

CONTRACT NO. NAS9-16097

PREPARED BY

W. C. LINDSEY
A. V. KANTAK
C. M. CHIE

LINCOM CORPORATION
P.O. BOX 2793D
PASADENA, CA 91105

MARCH 1981

TR-0381-1280

LinCom

TABLE OF CONTENTS

1. INTRODUCTION

The Solar Power Satellite offers a potentially economic means of producing solar based electric power which is virtually limitless in nature.

A critical requirement for the proposed Solar Power Satellite (SPS) concept is the ability of the satellite to beam and focus microwave energy to a predetermined spot located on the earth's surface from a geosynchronous orbit of 36,000 km. in altitude and with a transmission efficiency in excess of 90%. To form a coherent microwave beam to achieve the desired transmission efficiency a precise phase control of the EM wave during its passage through the entire circuit is necessary. The major elements required in the operation of an SPS system which employs retrodirectivity as a means of automatically forming and pointing the beam to the appropriate spot on the earth is shown in Figure 1.1. A block diagram representation of the system is shown in Figure 1.2.

As shown in the figure, the EM wave circuit includes: (1) the pilot transmitting antenna, (2) the power transmitting antenna on the satellite (spacetenna), and (3) the power receiving antenna on the earth (rectenna). The pilot transmitting antenna, situated at the center of the rectenna emits a pilot tone which is used by the spacetenna to direct the high power beam so that it comes to focus at the rectenna.

As mentioned earlier, the phase control of the EM wave is of paramount importance for the proper operation of the SPS system. Each block in the block diagram of Figure 1.2 is a potential phase disturbance source. From previous work on the SPS system it is agreed that a total phase error of 10^{0} at the spacetenna radiation ports would

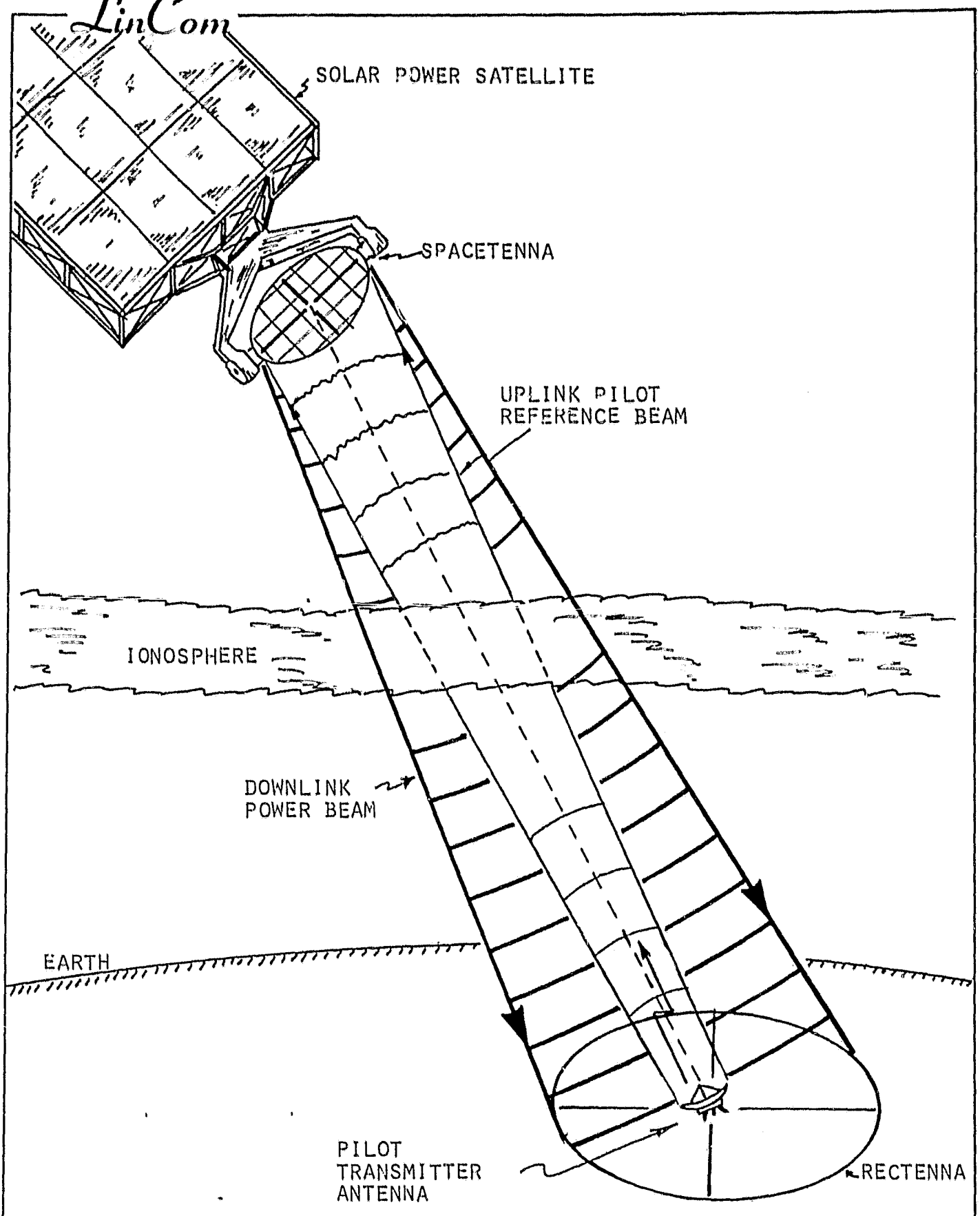

Fig. 1.1. ELEMENTS OF SOLAR POWER SATELLITE SYSTEM

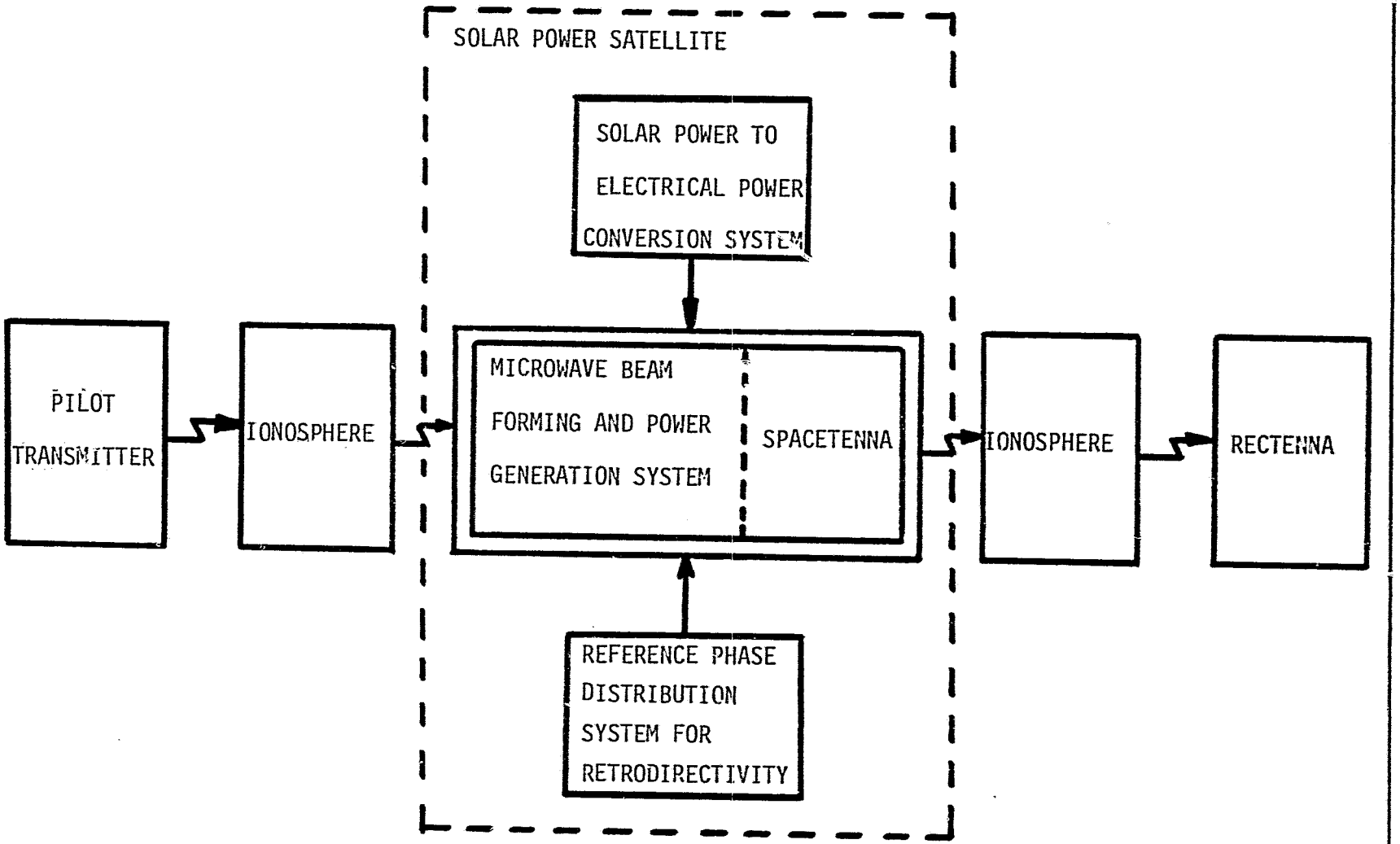

Fig. 1.2. SOLAR POWER SATELLITE SYSTEM BLOCK DIAGRAM

allow one to obtain an acceptable transmission efficiency in excess of 90%. The breakdown of the phase error in terms of all the potential sources of phase error in the SPS system so that the RMS phase error at the spacetenna radiation port is not greater than 10^{o} is shown in Figure 7.2. Subsequent sections describe each source of phase error and give the performance leading to selection of the allowable phase errors for the sources.

The executive summary of accomplishments and pertinent results is organized into five sections, each one is summarized as follows.

2. PILOT TRANSMITTER

The SPS MPTX system is deemed to have a retrodirective self cohering antenna system working with a pilot beam from the rectenna center. The pilot waveform will be a NRZ pseudonoise code amplitude modulated onto a subcarrier of 40 MHz. This subcarrier amplitude modulates the uplink carrier at 2.45 GHz. The pilot transmitter system functional block diagram is depicted in Figure 2.1.

The purpose of spread spectrum code modulation is several fold. First it provides link security, second it provides a multiple access capability for the operation of a network of SPSs and third, the antijamming protection is provided for both intentional radio frequency interference (RFI) and unintentional RFI such as those arising from neighboring SPS on an adjacent orbit.

Fig. 2.2 shows the spectrum of the uplink CW pilot tone. The subcarrier modulation shifts the spectrum of the NRZ PN code by 40 MHz on either side of the uplink carrier frequency of 2.45 GHz suppressing the carrier component. This shifting of the code spectrum is used to effectively reduce the noise at the output of the front end of the MPTX

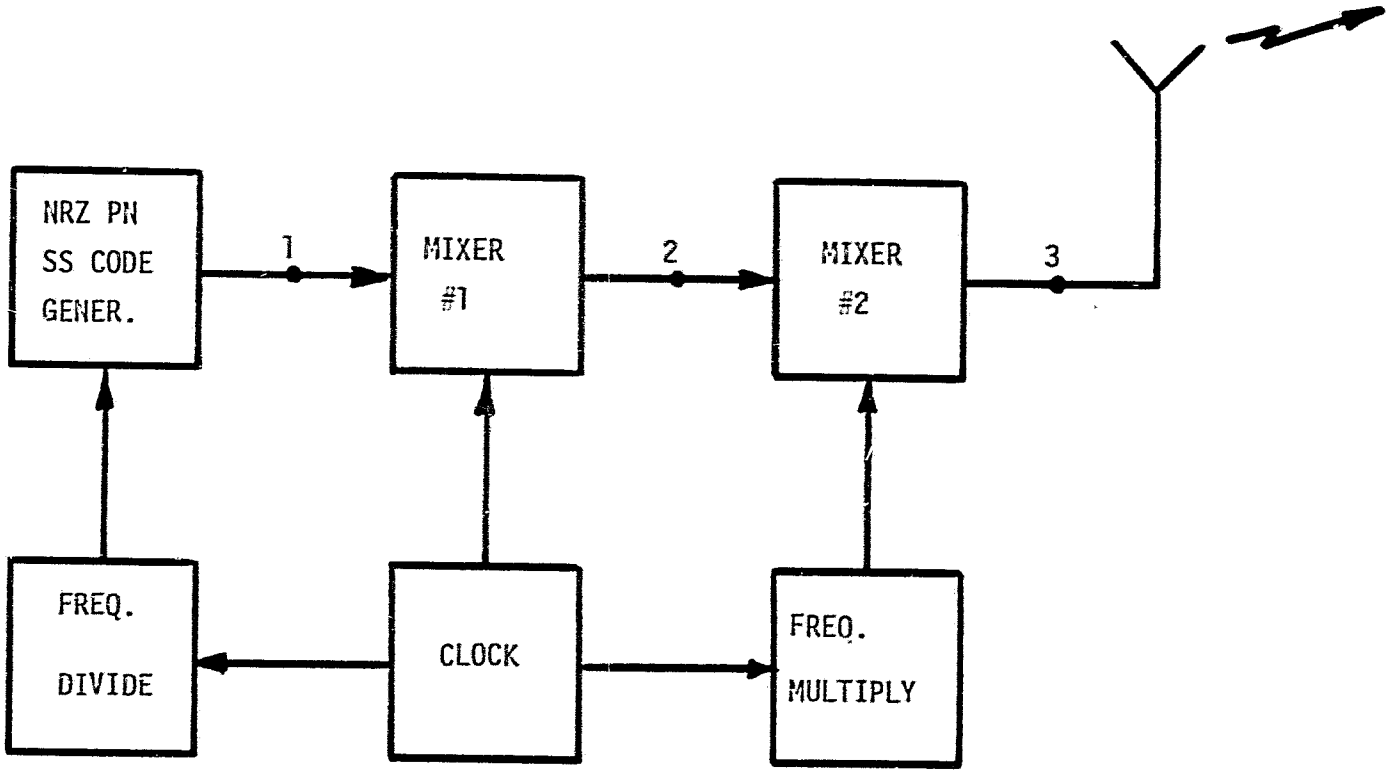

Fig. 2.1. Reference System Pilot Signal Transmitter Functional Diagram.

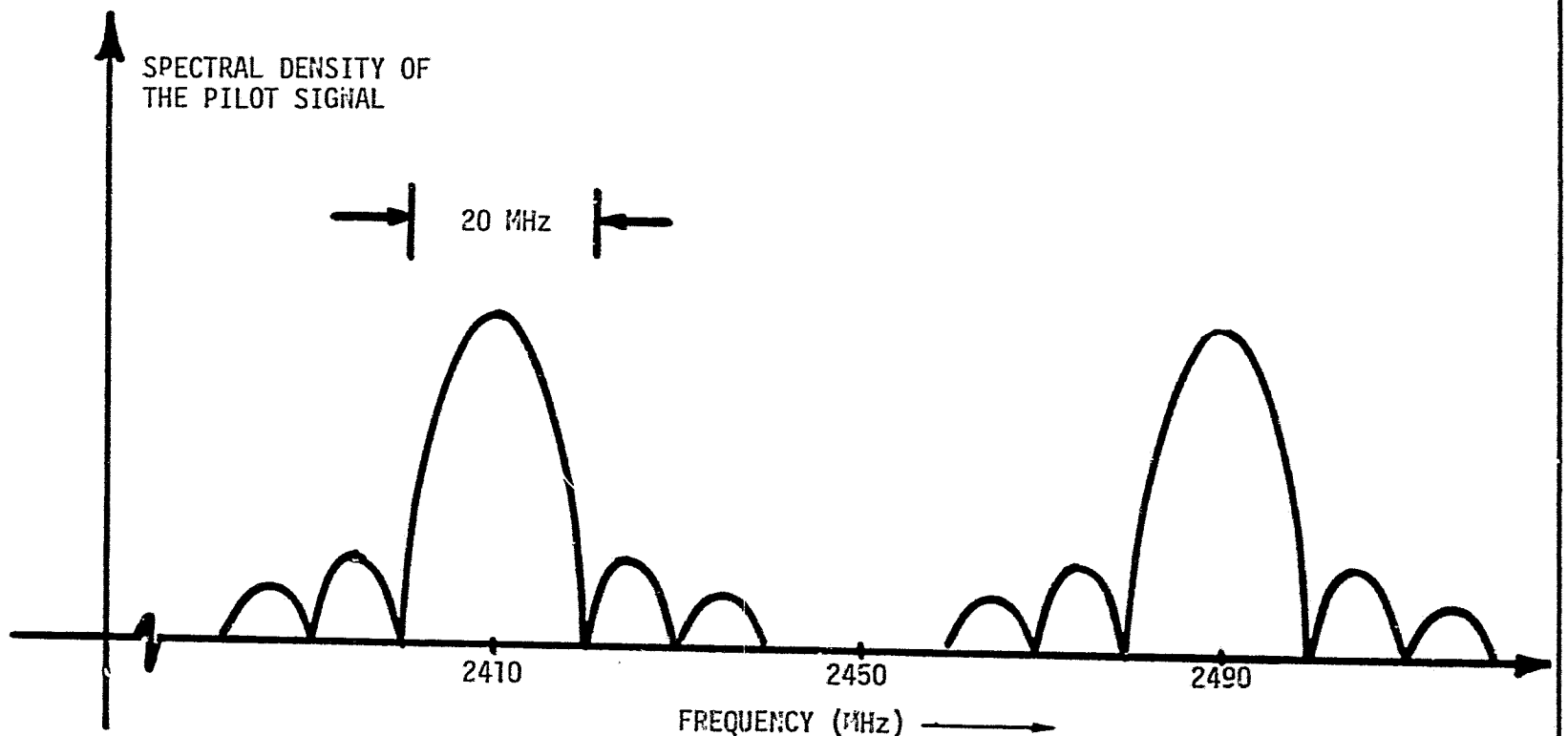

Fig. 2.2. SPECTRUM OF THE UPLINK PILOT WAVE.

system. On the MPTX system the suppressed carrier is regnerated, its phase is used to form the self cohering retrodirected downlink power beam.

As can be seen from the Fig. 2.1 the clock phase noise as well as the noise added by the system component will have a corresponding phase jitter introduced in the uplink pilot beam. This phase jitter constitutes one part of the total phase jitter suffered by the entire system. A list of parameter selection for the pilot signal is included in a later article.

The phase jitter added by the pilot transmitter to the pilot is required to be less than 1^{0}. As we will see later, phase jitter in the microwave radiating system is one major cause of loss of power transfer efficiency of the Solar Power Satellite.

3. IONOSPHERICS

The downlink power beam of the proposed SPS at geosynchronous altitude is to be formed by the retrodirective phase conjugation technique. The uplink pilot beam providing the phase information to the conjugator circuit passes through the heated ionosphere introducing the phase jitter to the phase of the pilot wave.

The heating produced by the downlink pilot beam would be of the underdense type, i.e., it is a case of heating of plasma with a microwave frequency greater than the critical frequency of the plasma, so that the heating wave penetrates the ionosphere. This underdense heating of the ionosphere creates irregularities in the ionsophere termed striations. The striations size depends on the angle between downlink power beam and the magnetic field of the plasma. Because of the horizontal dimension of the SPS beam in the ionosphere is about 5

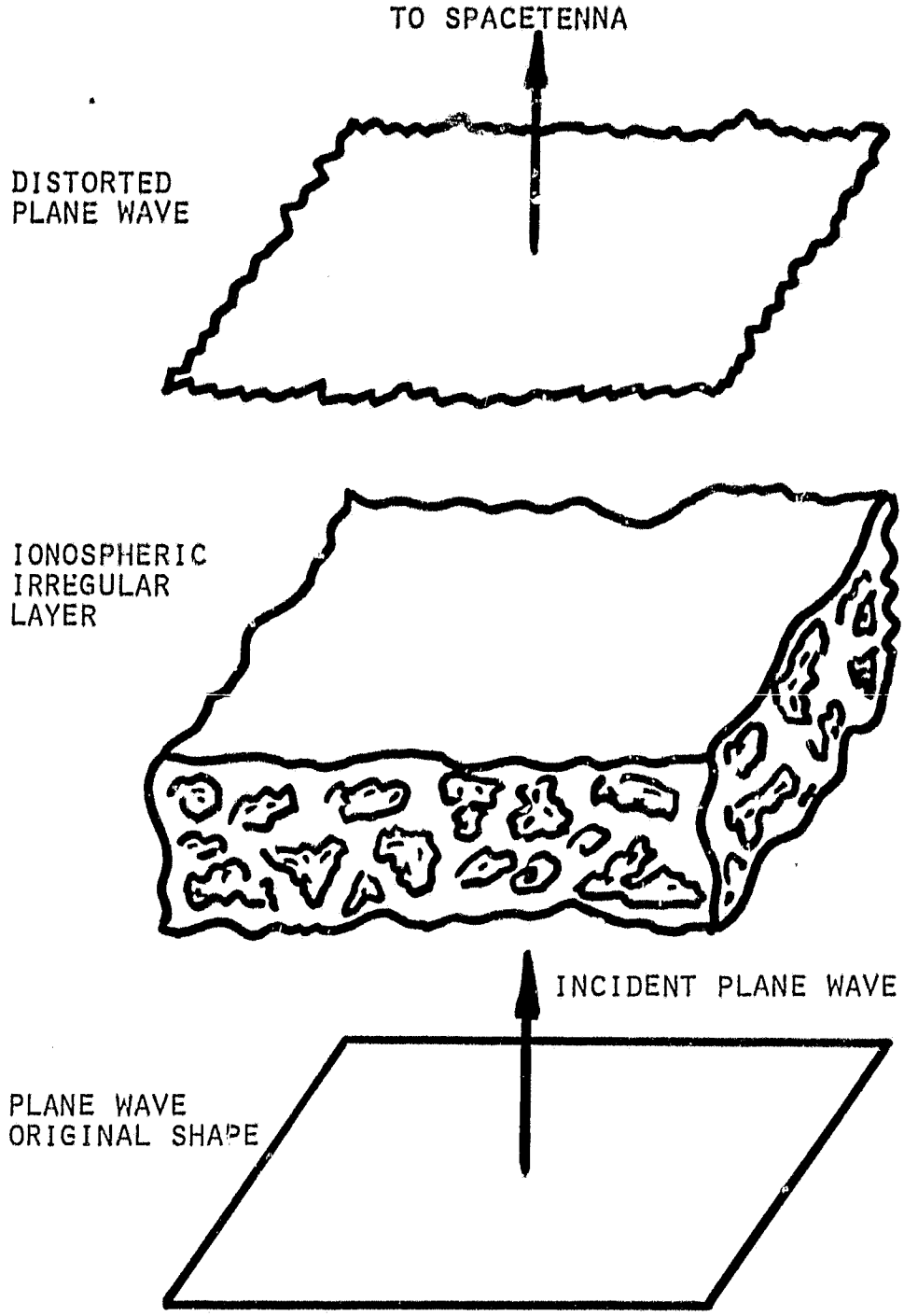

FIGURE 3.1. GEOMETRY OF SCINTILLATION PROBLEM.

Km, the striations of width 5 Km or less would be of any concern to the SPS uplink pilot beam. If the ionospheric irregularities have scales equal to or less than the Fresnel zone associated with the pilot beam then the diffractive scattering of the pilot beam will occur while if the scales are larger than the Fresnel zone the refractive scattering will dominate diffractive scattering.

Fig. 3.1 illustrates that in the presence of fluctuations of ionospheric electron concentration an impinging plain wave suffers phase fluctuations as it emerges from the striation layer. For small electron density fluctuations the emerging uplink pilot undergoes only phase fluctuations without any fluctuations in the intensity. As the wave front propagates towards the spacetenna, the phase mixing occurs and as a direct consequence, the spatial intensity fluctuations may also develop.

These processes affecting the phase of the uplink pilot are largely unknown and hence a need for experimentation exists. However from whatever data at hand it seems reasonable to assume a maximum phase jitter of 3^{o} on the uplink pilot received at spacetenna conjugation ports.

4. MASTER SLAVE RETURNABLE TIMING SYSTEM (MSRTS)

As mentioned earlier, solar power satellite employs retro-directivity as the means of automatically forming and pointing the high power microwave downlink beam to the rectenna site. The need for a constant phase reference necessary for the retrodirective operation of the spacetenna is comprehended by the reference phase distribution system shown in Fig. 4.1.

SPS PHASE CONTROL SYSTEM

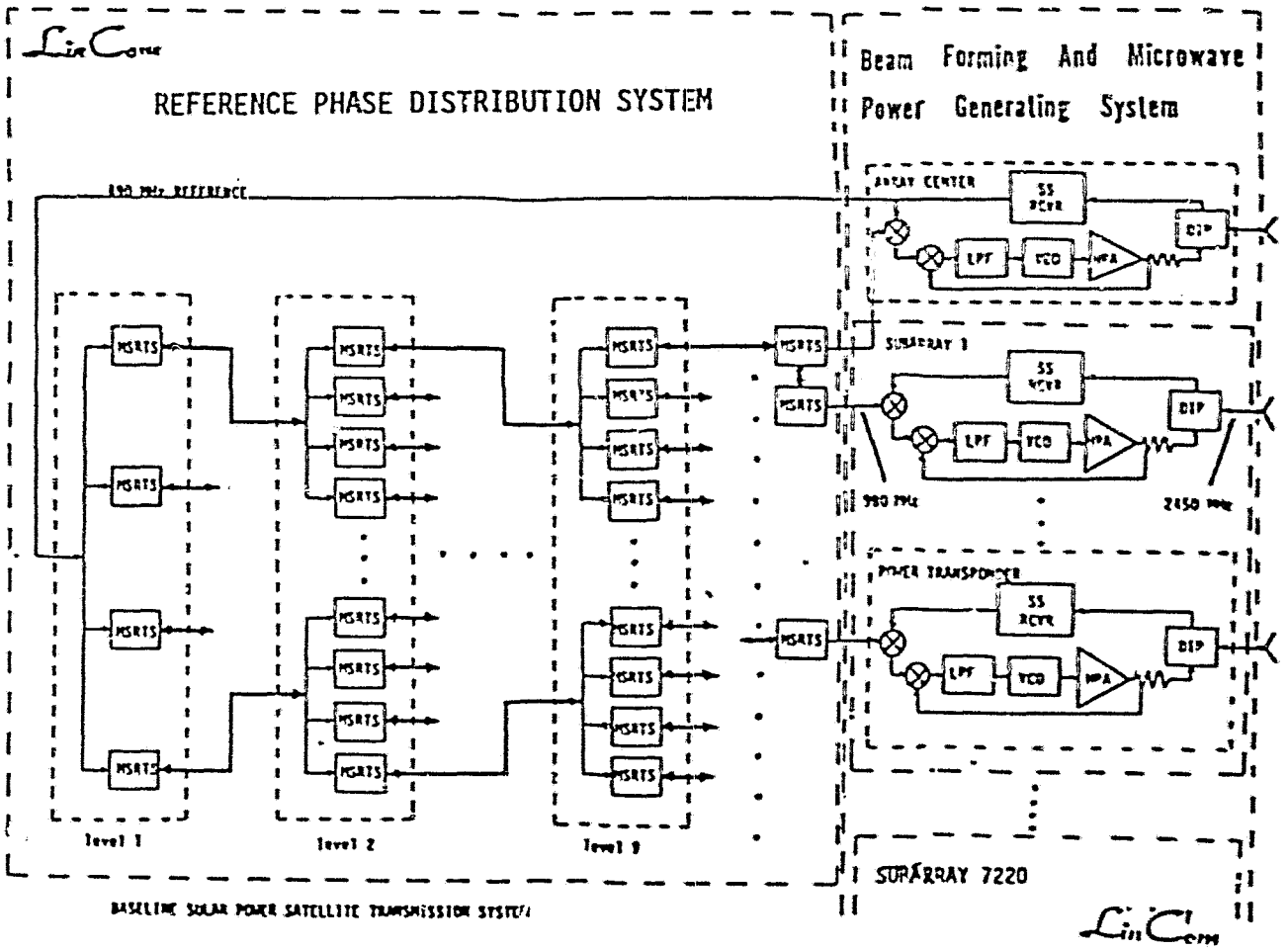

Fig. 4.1. SPS PHASE CONTROL SYSTEM.

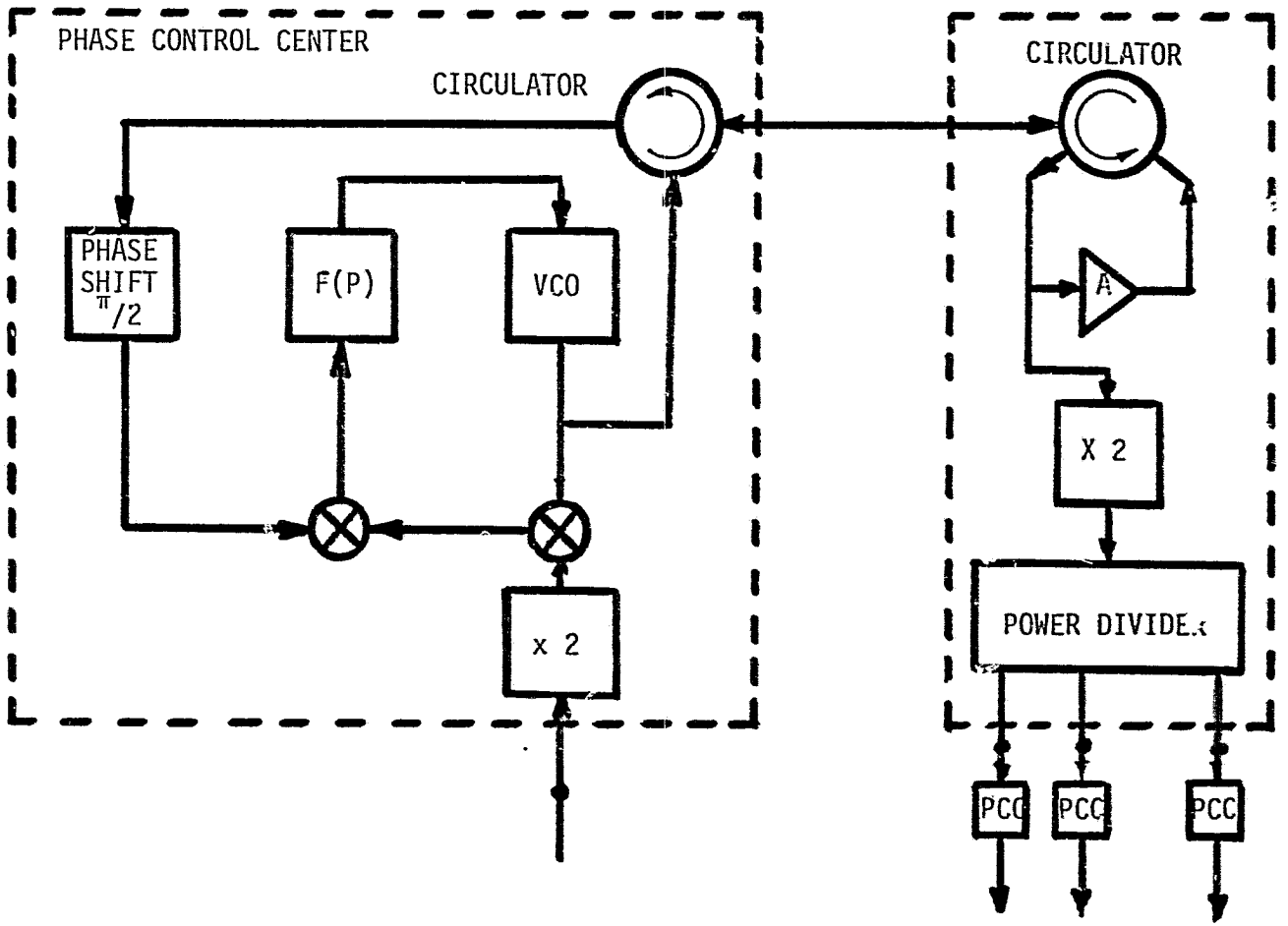

Fig. 4.2. MASTER SLAVE RETURNABLE TIMING SYSTEM

The reference phase distribution system is implemented in the form of a phase distribution tree structure. This tree is deemed to have four levels having 16, 16, 16, and 25 branches per each node at levels 1, 2, 3 and 4 respectively. The major purpose of the tree structure is to electronically compensate for the phase shift due to the transition path lengths from the center of the spacetenna to each phase control center (PCC) in each subarray. From which the constant phase is fed to each receiver for the purpose of conjugation. The electronic phase compensation is accomplished using the master slave returnable timing system (MSRTS) technique.

Figure 4.2 shows the electronic components of the MSRTS system in block diagram form. The master signal at the center of the spacetenna is fed to the frequency doubler at point A in the figure. The master phase is regenerated at point B which is frequency doubled and then is used to supply the regenerated master phase to the phase control centers in the next level in the phase distribution tree.

The MSRTS phase distribution system has several components such as the pilot signal receiver at the center of spacetenna, power splitters in the phase distribution tree, oscillators in the MSRTS, etc., each component adding to the phase jitter of the radiated power wave. The total rms phase jitter of the system is required to be less than 7.5^{o}. This is the phase jitter observed at the input of the conjugator at each power amplifier tube. The phase jitter below 7.5^{o} will be required to achieve power transfer efficiency of in excess of 90%.

5. SPS RECEIVER

The basic idea behind the SPS receiver is to receive the uplink pilot, regenerate the suppressed carrier and use the phase of the

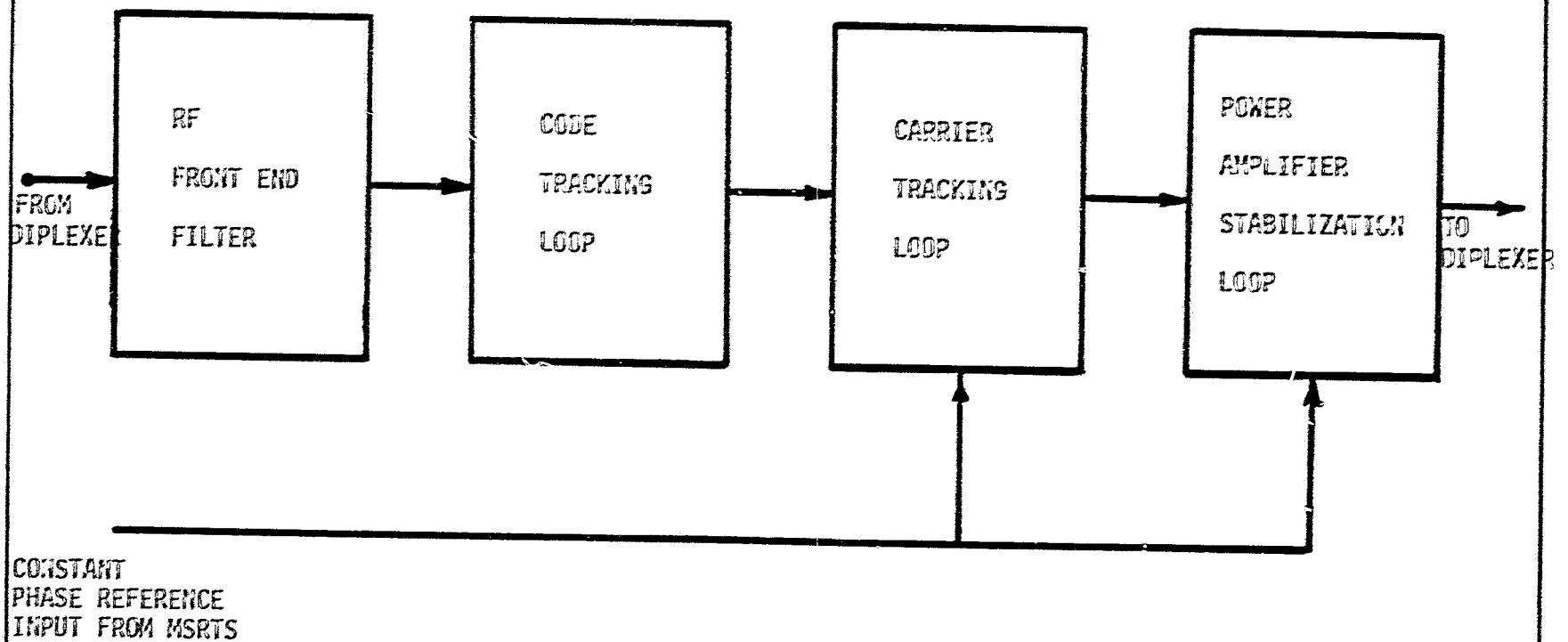

Fig. 5.1. SPS MPTX SYSTEM

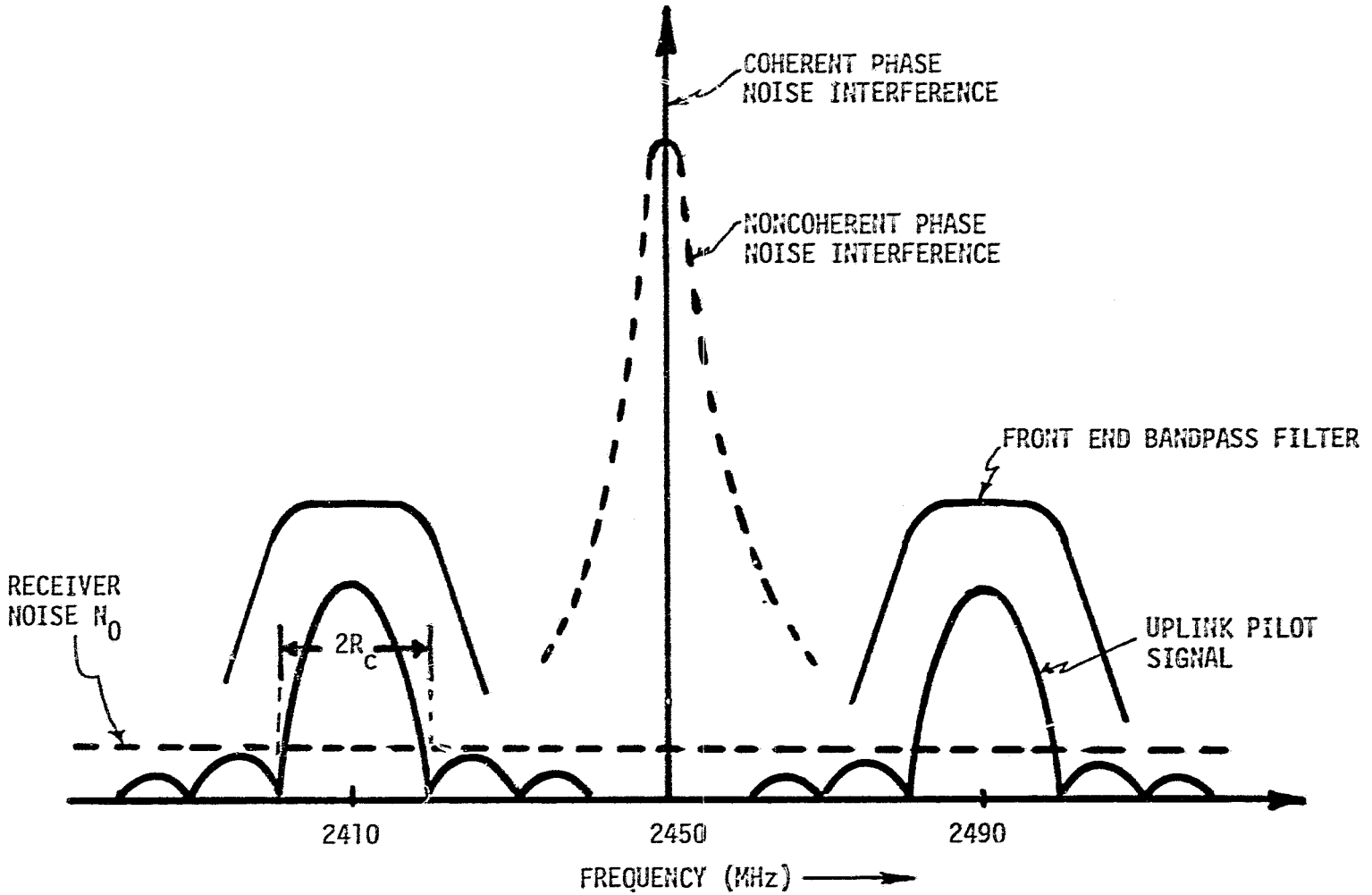

Fig. 5.2.SIGNAL AND NOISE SPECTRUM INTO MPTX TRANSPONDER

carrier into the conjugation process to beam down the microwave power. Figure 5.1 shows the basic loops required in the receiver in block diagram form. These loops are (1) the code tracking loop (PN despreader loop), (2) the carrier tracking loop (pilot phase tracking loop) and (3) the PA phase control loop. Analytical models for the above loops as well as the front end filter performance are formulated.

The signal and noise spectra at the input to the transponder are shown in Fig. 5.2. The signal plus noise is filtered by the front end filter. The filter is of notch type and the main purpose of it being to pass the NRZ PN spread pilot signal sidebands without distortion at the same time rejecting the self and mutual coupling noises affecting the performance of the transponder. Figure 4.2 illustrates the amplitude response of the front end filters.

The filtered signal plus noise is then fed to the code tracking loop. The code tracking loop is one chip time tau-dither loop which sequentially correlates the retarded and advanced versions of locally generated code with the incoming code. The error after passing through the arm filter drives the loop VCO which controls the local code generation. When the loop locks, the error between the incoming code and the local code is negligible (there is no message on the code). The loop bandwidth and the arm filter bandwidth are of importance in determining the code tracking error. Following table on page 17 gives the values selected for these parameters.

Output of the front end filter is also fed to the carrier tracking loop. The main function of this loop is to reproduce the suppressed carrier and track its phase. The phase fluctuations at the output of this loop is directly related to the various noise processes through the

closed loop transfer function of the loop. The important parameters determining the performance of the loop are the chip rate of the code, the front end filter bandwidth and the phase lock loop bandwidth. A computer program termed SOLARSIM is developed to enable performance tradeoffs for the entire solar power satellite system and the recommended values for the pertinent design parameters of the receiver are given in a table later on.

6. HIGH POWER AMPLIFIER

The dc to microwave conversion unit is the high power amplifier. Fig. 4.1 shows the position of the high power amplifier in the phase control hierarchy. The output of phase conjugation circuits serve as inputs to the high power amplifier. The klystron amplifier in the power transponder generates a phase noise profile that can add significantly to the downlink carrier phase error if it is unattended for. Phase noise added by the power amplifier can be reduced to acceptable levels if one puts a stabilization loop around the amplifier as shown in Fig. 4.1

The loop around the klystron amplifier tracks the noise components around the carrier frequency. Only those noise components which have Fourier frequencies greater than the loop bandwidth will be transmitted to the power beam. When the phase noise rejection is our only consideration, the obvious solution is to widen the loop bandwidth as much as possible but this also opens up the bandwidth for other noises in the transponder. Recommended value for the bandwidth is given in the table later on.

7. SUMMARY OF RESULTS

The important findings on the pilot transmitter and spacetenna transponder design parameters can be summarized as follows:

Pilot Transmitter

- EIRP = 93.3 dBW
- PN Chip Rate = 10 Mcps
- Chip Time = 0.1 μsec
- Code Repeats After 10,000 bits

Front End

- 6 Pole Butterworth Bandpass Filters
- Center Frequencies = 2410 MHz and 2490 MHz
- 3 dB Bandwidth = 20 MHz
- 3 dB Notch Bandwidth = 40 MHz

Code Tracking Loop

- 6 Pole Butterworth Bandpass Arm Filter
- 3 dB Bandwidth - 3 kHz
- Code Loop Bandwidth = 10 Hz
- Phase Jitter of Code Tracking Loop $\leq$ 1% Chip Time

Carrier Tracking Loop

- 3 dB Bandwidth of the High Pass Filter = 20 MHz
- Carrier Loop Bandwidth = 10 Hz
- Phase Jitter of Carrier Tracking Loop $\leq 0.4^{o}$

Power Amplifier Stabilization Loop

- Loop Bandwidth $\geq$ 10 kHz

In arriving at these values, we have extensively used the capabilities of SOLARSIM to perform the necessary tradeoffs. These

Figure 7.1 Phase Error Budget for the SPS System

PILOT TRANSMITTER	IONOSPHERE	PHASE DISTRIBUTION SYSTEM (MSRTS)	SPREAD SPECTRUM RECEIVER	HIGH POWER AMPLIFIER	IONOSPHERE
•PILOT TRANSMITTER VCO JITTER = 1°	•REFRACTIVE SCATTERING •REFLECTIVE SCATTERING •UNDERDENSE HEATING	•PILOT RCVR VCO JITTER (3°) •POWER SPLITTER IN PHASE DISTRIBUTION TREE (6°) •PHASE JITTER OF VCO's IN THE PHASE DISTRIBUTION TREE (2.4°) •UNCOMPENSATED PATH DELAY (2.4°)	•PHASE JITTER DUE TO CARRIER TRACKING LOOP •PHASE JITTER DUE TO CODE TRACKING LOOP DUE TO NOISE •PHASE JITTER DUE TO VCO IN THE LOOPS	•PHASE JITTER DUE TO THE HPA STABILIZATION LOOP (5°)	•IONOSPHERE OF DOWNLINK POWER BEAM
PHASE JITTER 1°	PHASE JITTER 3°	RMS PHASE JITTER = 7.5°	RMS PHASE JITTER = 3°	PHASE JITTER 5°	PHASE JITTER 0°

TOTAL RMS PHASE JITTER = 10°.

POWER TRANSFER EFFICIENCY ≅ 91°

results are generated using a model of RFI with coupling coefficients of -20 dB for the self as well as mutual coupling of the radiators.

Every item in the SPS system described in above pages introduces a phase jitter to the phase of the downlink power beam. This phase jitter is one primary cause of degradation of power transfer efficiency. There are other efficiency degrading effects such as antenna tilts, tilt jitters, radiating and conjugation point jitter to name a few. Fig. 7.1 shows the contribution of system components to the phase jitter suffered by the downlink power beam and the resulting power transfer efficiency from it. In the calculation of power transfer efficiency the other efficiency degrading effects than the phase noise are held to zero.

Figure 7.2 shows the power transfer efficiency as a function of the total rms phase error. As can be seen from this figure, at 10.5^{o} of phase jitter the efficiency is about 90.5%.

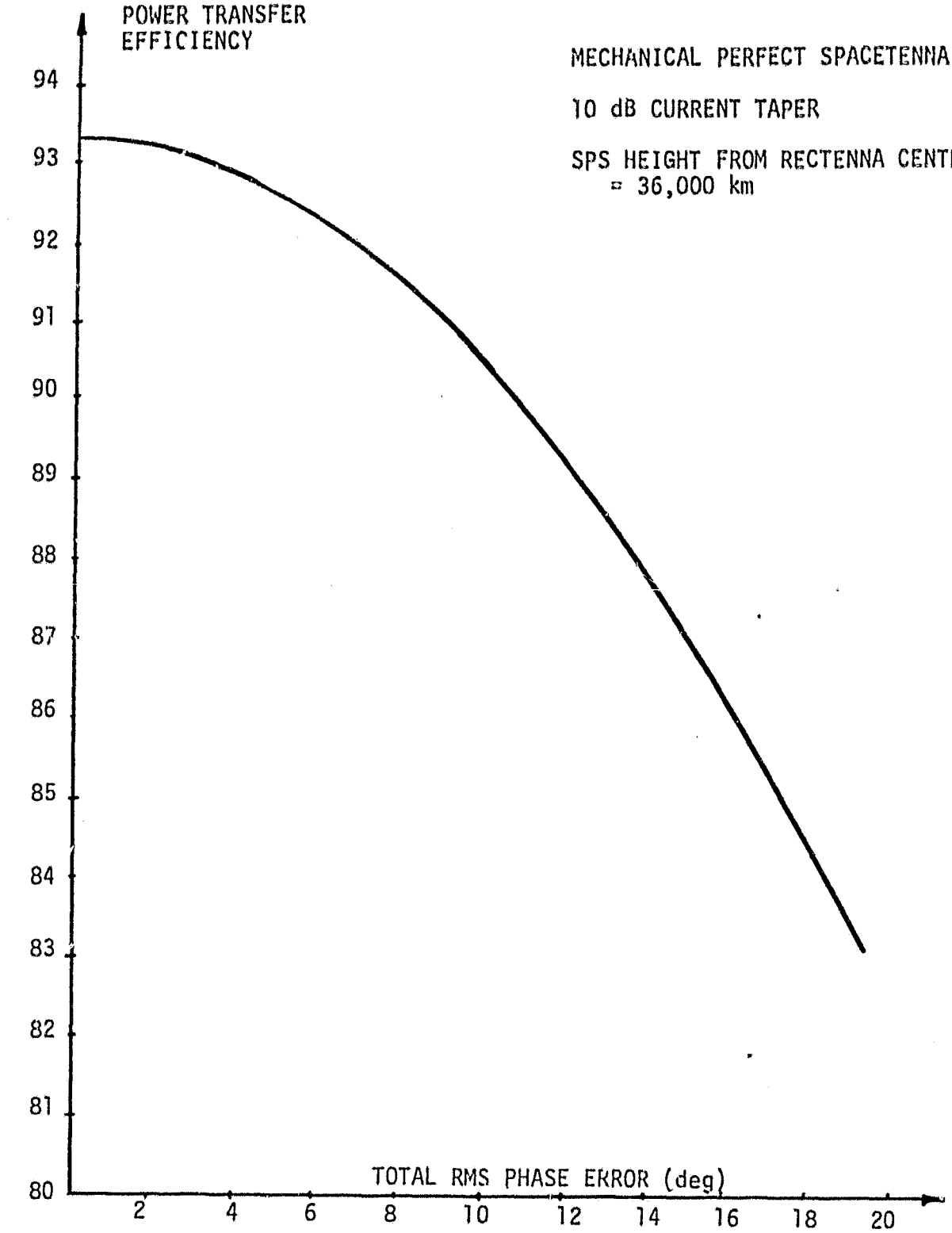

Fig. 7.2. SPS Power Transfer Efficiency vs the Total rms Phase Error.